

First-principles calculation of the plasmon resonance and of the reflectance spectrum of Silver in the GW approximation

Andrea Marini,¹ Rodolfo Del Sole,¹ and Giovanni Onida^{1,2}

¹ *Istituto Nazionale per la Fisica della Materia, Dipartimento di Fisica dell'Università di Roma "Tor Vergata"*

² *Istituto Nazionale per la Fisica della Materia, Dipartimento di Fisica dell'Università di Milano, Via Celoria 16, I-20133 Milano, Italy*

(Dated: October 28, 2018)

We show that the position and width of the plasmon resonance in Silver are correctly predicted by ab-initio calculations including self-energy effects within the GW approximation. Unlike in simple metals and semiconductors, quasiparticle corrections play a key role and are essential to obtain Electron Energy Loss in quantitative agreement with the experimental data. The sharp reflectance minimum at 3.92 eV, that cannot be reproduced within DFT-LDA, is also well described within GW . The present results solve two unsettled drawbacks of linear response calculations for Silver.

PACS numbers: 71.15.-m, 71.45.Gm, 79.20.-m

I. INTRODUCTION

Although the coexistence of quasiparticles and collective excitations in an interacting system is well known, our knowledge of their properties and mutual interactions in real materials is far from being complete. One of the most successful approaches to the calculation of the quasiparticle (QP) band structure for a wide range of materials is the GW method¹. Starting from a non-interacting representation of the system, electrons and holes are screened by the surrounding electronic clouds created through the Coulomb interaction. This description has been shown to be rather general in describing direct and inverse photoemission spectra, also for complicated systems as reconstructed surfaces and clusters^{2,3}. Noble metals, on the other hand, have been studied only very recently. Full quasiparticle calculations have been carried out only for Cu obtaining an excellent agreement with the experimental band structure⁴. Collective modes, i.e. plasmons, occur at energies for which the real part of the dielectric function vanishes with a corresponding small imaginary part; they can be observed experimentally as sharp peaks in Electron Energy Loss Spectra (EELS). A well established technique to calculate EEL spectra uses the single particle or random phase approximation (RPA) for the polarization function, obtained in terms of Ab-Initio energy bands. The latter can be calculated within the Kohn Sham (KS)⁵ formulation of Density Functional Theory⁶ in the Local Density Approximation⁷ (DFT-LDA) or in the Generalized Gradient Approximation (GGA)⁸, when the exchange-correlation potential V_{xc} is considered as an approximation to the self-energy operator Σ . This approach completely neglects self-energy corrections, that is the difference $\Sigma - V_{xc}$, and excitonic effects, whose inclusion has been faced only recently. In the case of silicon, Olevano and Reining⁹ showed that using the quasiparticle energy bands without including excitonic effects the shape of the plasmon peak worsens with respect to the experiment. Inclusion of self-energy corrections and excitonic effects

yields a spectrum very similar to DFT-LDA one and to the experiment. Ku and Eguiluz¹⁰ obtained a correct positive dispersion of the plasmon width in K using the single particle approximation, with no many-body corrections beyond DFT-LDA. In these cases many-body effects (quasiparticle corrections and/or excitonic effects) are not required to describe correctly the experimental data. These results agree with the general feeling that excitonic effects partially cancel self-energy corrections. A similar result has been found for Cu^{11,12}, where the RPA response function calculated without many-body corrections yields good agreement with the experimental EEL and optical spectra.

In this framework the case of Silver is rather surprising: the experimental EELS is dominated by a sharp plasmon peak at 3.83 eV¹³, whose position and width are badly reproduced in DFT-LDA RPA¹⁴. In particular, a width of about 0.5 eV is obtained within this approach, to be contrasted with a much narrower experimental width (~ 100 meV). A similar discrepancy occurs in the reflectance spectrum, where a very narrow dip at 3.92 eV is hardly reproduced by DFT-LDA calculations. Some papers have recently appeared^{15,16} which correct DFT-LDA results by empirical scissors-operators shifts (or similar), meant to better account for the band structure. Improved dielectric functions are obtained in this way, but no solution of the puzzles mentioned above has been given.

In Sec. II we show that non trivial quasiparticle corrections on the highly localized d bands strongly modify the absorption spectrum threshold. As a consequence, in Sec. III we show that the plasmon position and width are renormalized by quasiparticle effects leading them close to the experimental values. Also the reflectance dip at 3.92 eV turns out to be well described in the same scheme. Finally in Sec. IV we summarize our conclusions.

II. QUASIPARTICLE EFFECTS ON THE ABSORPTION SPECTRUM

We proceed calculating the band structure of Silver within DFT-LDA. The diagonalization of the KS hamiltonian is performed using norm-conserving pseudopotentials (PPs) and a plane waves basis¹². The use of soft (Martins-Troullier¹⁷) PPs allows us to work at full convergence with a reasonable kinetic energy cutoff (50 Ry.). Many-body corrections are added on top of the DFT-LDA band structure following the implementation of the GW method described in Ref.⁴. The resulting quasiparticle band structure of Ag at high symmetry points is compared with DFT-LDA results in Table I. While the deeper energy levels remain mostly unchanged, a downward shift of about 1.3 eV of the top *d* bands leads to a decrease of the bandwidth, and hence to an excellent agreement with experiment. The residual discrepancies between the position of the GW bands and the experimental results (~ 0.2 eV) is larger than in the case of copper⁴ (~ 0.05 eV). This is a consequence of the QP renormalization of the Fermi level in silver (~ 0.6 eV), not present in copper, which yield the large QP corrections reported in Table I and an additional error. Differently from semiconductors, GW corrections *do not* act as a rigid shift of the whole occupied band structure with respect to the empty (conduction) part. QP corrections are highly non trivial since even their sign turns out to be band/*k*-point dependent, as we have already shown in the case of copper⁴.

		DFT-LDA	GW	Experiment
Positions	Γ_{12}	-3.57	-4.81	-4.95
of	X_5	-2.49	-3.72	-3.97
<i>d</i> -bands	$L_3(2)$	-2.71	-3.94	-4.15
	$\Gamma_{12} - \Gamma_{25'}$	1.09	0.94	1.11
Widths	$X_5 - X_3$	3.74	3.39	3.35
of	$X_5 - X_1$	3.89	3.51	3.40
<i>d</i> -bands	$L_3(2) - L_3(1)$	1.98	1.85	1.99
	$L_3 - L_1$	3.64	3.17	2.94
	$X_5 - X_2$	0.27	0.29	0.38

TABLE I: Theoretical band widths and band energies for silver, at high-symmetry points. GW energies are relative to the QP Fermi Level. The striking agreement with the experimental results shows that the silver band-structure is very well described at the GW level. The values in the last column are taken from Ref.²⁴ where spin-orbit splittings have been removed by making degeneracy-weighted averages.

To calculate the EEL spectra, we use the QP band structure to evaluate the inverse dielectric function $\epsilon^{-1}(\omega)$ ¹⁹:

$$\epsilon^{-1}(\omega) = \left[\epsilon_{ib}(\omega) - \frac{\omega_D^2}{\omega(\omega + i\eta)} \right]^{-1}, \quad (1)$$

where $\epsilon_{ib}(\omega)$ is the interband contribution and $\omega_D = 9.48$ eV is the Drude plasma frequency, both calculated Ab-Initio following the procedure described in Refs.^{12,18}. The interband RPA dielectric function is given by

$$\epsilon_{ib}(\omega) = 1 - 4\pi \lim_{\mathbf{q} \rightarrow 0} \int_{BZ} \frac{d^3\mathbf{k}}{(2\pi)^3} \sum_{n \neq n'} \frac{|\langle n'|\mathbf{k} - \mathbf{q}|e^{-i\mathbf{q}\cdot\mathbf{r}}|n\rangle|^2}{|\mathbf{q}|^2} \frac{f_{n',\mathbf{k}-\mathbf{q}} - f_{n,\mathbf{k}}}{\omega + E_{n,\mathbf{k}} - E_{n',\mathbf{k}-\mathbf{q}} + i\eta}, \quad (2)$$

where $0 \leq f_n(\mathbf{k}) \leq 2$ represents the occupation number summed over spin components. $\eta = 0.1$ eV has been used in the present calculations. The $\mathbf{q} \rightarrow 0$ limit of Eq. (2) has been done including the effects of the pseudopotential non-locality, as done in Ref.¹². The GW optical-transition energies ($E_{n,\mathbf{k}} - E_{n',\mathbf{k}}$) are obtained fitting the QP corrections calculated at 29 *k*-points of a regular grid in the irreducible Brillouin zone (BZ). Separate fitting curves (shown in Fig. 1) have been used for selected band pairs (*n, n'*) and *k* regions in the BZ, in order to correctly reproduce the energy dependence of the quasiparticle corrections.

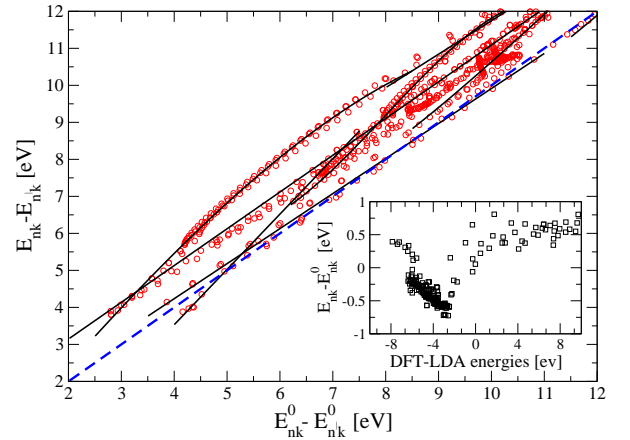


FIG. 1: GW optical-transition energies (circles) plotted as a function of DFT-LDA ones for a regular grid of 29 *k*-points in the irreducible Brillouin zone. The dashed line corresponds to vanishing GW corrections while full lines are our fitted curves. They are used to extend the GW corrections to the optical transition energies of a larger *k*-points grid. GW corrections shift upward the electron-hole energies, except for some transitions between 4 and 5 eV (as discussed in the text). In the inset GW corrections are shown versus DFT-LDA energies.

From Fig. 1 it is evident that GW corrections are highly non-trivial (ranging from -0.75 to 0.5 eV for filled states, and from 0 to 0.75 eV for empty states, as shown in the inset). GW optical-transition energies are generally above the dashed-line, representing the condition of vanishing quasiparticle corrections ($E_{n,\mathbf{k}} - E_{n',\mathbf{k}} = E_{n,\mathbf{k}}^0 - E_{n',\mathbf{k}}^0$), and lead to upward

shifts of the electron-hole energies. However between 4 and 5 eV some electron-hole energy shifts are negative. These correspond to transitions close to the L point from the Fermi level to the 7th (empty) band.

In Fig. 2 the GW interband contribution $\epsilon''_{ib}(\omega)$ is compared with the DFT-LDA result. In the upper panel all the transitions except those involving the \mathbf{k} -points near the L point are included: GW corrections shift the whole spectra to *higher* energies, with the threshold energy occurring at ~ 4 eV, in agreement with experiment. In panel (b) we consider the transitions (sketched in the inset) not included in panel (a). At difference with panel (a), GW shifts the DFT-LDA spectrum toward *lower* energies. In conclusion, weak interband transitions start at the threshold in panel (b) (3.36 eV), while the main onset of $\epsilon''_{ib}(\omega)$ is that of panel (a), ~ 4 eV. The resulting (total) dielectric function is shown in the inset of Fig. 3.

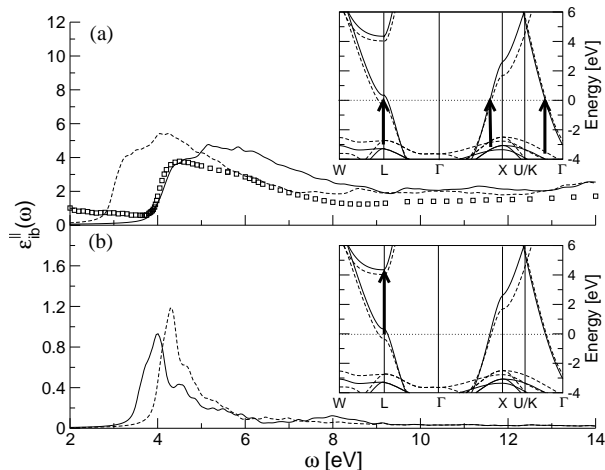


FIG. 2: Interband absorption spectrum $\epsilon''_{ib}(\omega)$ of Ag calculated using the quasiparticle GW band structure. Theoretical spectra do not contain the intraband contribution. In both panels and insets: solid line, GW; dashed line, DFT-LDA. Only in panel (a): boxes, full experimental $\epsilon''(\omega)$ ²². In panel (a) all the transitions except those involving the \mathbf{k} -points near the L point are included. These are considered separately in panel (b). In the insets the DFT-LDA band structure is compared with the GW result, and the arrows indicate the most important transitions involved near the absorption threshold. In panel (b) quasiparticle corrections shift some transition energies at the L point *below* the main threshold of panel (a). These are responsible for the plasmon damping.

III. THE RENORMALIZED PLASMON FREQUENCY

The two different effects of GW corrections on $\epsilon''_{ib}(\omega)$ shown in Fig. 2 are crucial in determining the properties of the plasmon resonance whose frequency, ω_p , is defined

through the relation

$$\epsilon_{ib}(\omega_p) - \frac{\omega_D^2}{\omega_p^2} = 0. \quad (3)$$

ω_p is, in general, complex since decay into electron-hole pairs gives to the plasmon a width proportional to $\epsilon''_{ib}(\omega_p)$. Now, the sharp onset of $\epsilon''_{ib}(\omega)$ at ~ 4 eV (see inset of Fig. 3) is responsible for a solution of Eq. (3) at 3.56 eV, just below the main interband threshold. Within DFT-LDA, instead, the interband threshold of $\epsilon''_{ib}(\omega)$ at ~ 3 eV remains below ω_p , resulting in a strongly damped plasmon peak as shown in Fig. 3 (dashed line). From Fig. 2, panel (b), we see that the only transitions contributing to the plasmon width, proportional to $\epsilon''_{ib}(\omega_p)$, are those from the Fermi surface to the first conduction band at the L point. These decay channels are in agreement with many experimental results²⁰ that, using temperature and alloying techniques, have singled out the electron-hole transitions responsible for the plasmon damping.

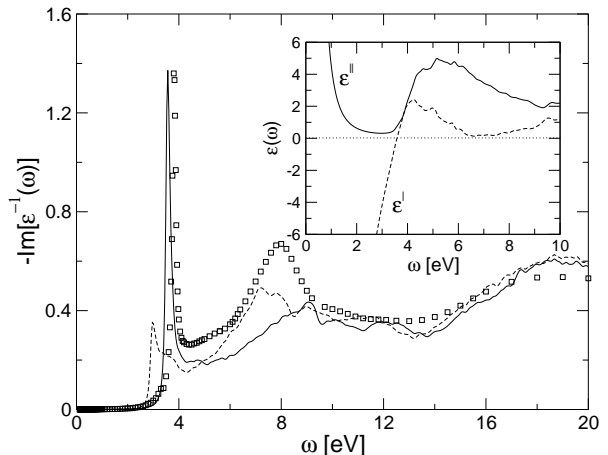


FIG. 3: Electron Energy Loss Spectrum (EELS) of Silver. Solid line: GW. Dashed line: DFT-LDA. Boxes: experiment²². The non trivial quasiparticle GW corrections improve considerably the DFT-LDA plasmon peak, yielding a striking agreement with the experiment. The GW dielectric function is shown in the inset.

GW-corrected EELS is compared with DFT-LDA and experimental results in Fig. 3: the plasmon peak, underestimated in intensity and position in DFT-LDA, is shifted toward higher energies and strongly enhanced by GW corrections, in striking agreement with experiment. In Fig. 2 an overestimation of the absorption spectrum with respect to the experiment is observed (similar to that found in Cu¹²). This is reflected in an underestimation of the loss intensity close to 8 eV, and might be due to the neglect of QP renormalization factors in Eq. (2) and to excitonic dynamical effects²¹. Despite this partial agreement in the 8 eV region, the present *Ab-initio* GW calculation is able to reproduce correctly the plasmon

resonance. This resonance can be interpreted as a collective (Drude like) motion of electrons in the partially filled band. However, according to Eq. 3, ω_p does not coincide with the bare Drude frequency ω_D , the difference arising from the screening of the electron-electron interaction by virtual interband transitions. The plasmon resonance, although blueshifted with respect to DFT-LDA, remains *below* the main interband threshold, but overlaps the weak low-energy tail of interband transitions (see Fig. 2, Frame (b)) acquiring a small –yet finite– width. The highly non-trivial QP shifts of interband transitions are crucial to obtain this result.

The polarization of the “medium” where the plasmon oscillates (the *d* electrons) is hence important to determine its energy and width. This polarization is absent in the homogeneous electron gas because there are no localized *d* orbitals and no interband transitions; it is weak in semiconductors (like Si), because interband transitions occur at energies far from that of the plasma resonance. The same polarization effect is present, but destructive in copper due to the lower onset of interband transitions. EELS peaks occur *above* this onset and are therefore strongly broadened. In conclusion, the delicate interplay of plasmon-frequency renormalization with the shift of the interband-transition onset, both due to QP corrections, may yield (in Silver) or may not yield (in Copper) a sharp plasmon resonance.

Another important quantity is the reflectance, $R(\omega) = (|N(\omega) - 1| / |N(\omega) + 1|)^2$, where N is the complex refraction index defined by $[N(\omega)]^2 = \epsilon(\omega)$. In Fig. 4 we compare the *GW* $R(\omega)$ with the DFT-LDA one, and with experimental results²². The latter shows a very narrow dip at 3.92 eV, close to the plasmon frequency, arising from the zero-reflectance point ω_0 , defined as $\epsilon(\omega_0) = 1$. Again, the width and depth of this reflectance dip are related to the imaginary part of $\epsilon(\omega)$. *GW* corrections make ω_0 to occur below the main onset of interband transitions, and hence produce a very narrow and deep reflectance minimum. Here the agreement between *GW* results and experiments for the intensity and width of the dip at 3.92 eV is even more striking than in the EELS.

This result is of great importance for the optical and EELS properties of Ag *surfaces*. Very recent calculations of Reflectance Anisotropy Spectra (RAS) within DFT-LDA for Ag(110)²³ were not able to reproduce quantitatively a sharp dip observed experimentally. This feature, at an energy $\omega_r = 3.8$ eV, has been assigned to a bulk resonance, arising in the RAS spectrum when $\epsilon(\omega_r) = 1$.

Hence, it is the same occurring in the reflectance spectrum of Fig. 4. Its width and shape are strongly related to the reflectance dip of Fig. 4, and therefore they need *GW* corrections to be well reproduced.

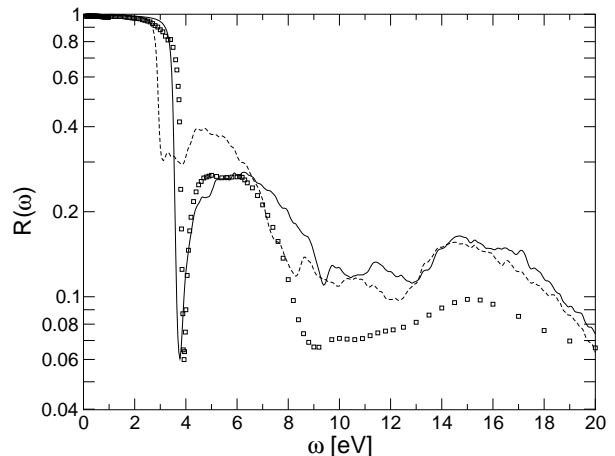


FIG. 4: Reflectivity spectrum of Silver. Solid line: *GW*. Dashed line: DFT-LDA. Boxes: experiment²². The experimental sharp dip at 3.92 eV is correctly reproduced by *GW*, with a substantial improvement on the DFT-LDA spectrum.

IV. CONCLUSIONS

We have performed a calculation of the EEL and reflectivity spectra of silver within the RPA approach, using the quasiparticle band structure calculated within the *Ab-Initio* *GW* method. We have shown that the peculiar, well known plasmon peak in the EELS and the deep reflectivity minimum observed experimentally, are quantitatively described by theory, for the first time without requiring adjustable parameters. Our theoretical calculations do not contradict previous results for semiconductors and simple metals (where many-body effects are less important) if the role played by *d* orbitals is correctly interpreted.

This work has been supported by the INFM PRA project “1MESS”, MURST-COFIN 99 and by the EU through the NANOPHASE Research Training Network (Contract No. HPRN-CT-2000-00167). We thank Angel Rubio and Lucia Reining for useful discussions.

¹ L. Hedin, Phys. Rev. **139**, A796 (1965).

² F. Aryasetiawan and O. Gunnarsson, Rep. Prog. Phys. **61**, 237-312 (1998).

³ See e.g.: W.G. Aulbur, L. Jönsson and J.W. Wilkins, Solid State Physics **54**, 1 (1999).

⁴ A. Marini, G. Onida and R. Del Sole, Phys. Rev. Lett. **88**, 016403 (2002).

⁵ W. Kohn and L. J. Sham, Phys. Rev. **140**, A1113 (1965).

⁶ P. Hohenberg and W. Kohn, Phys. Rev. **136**, B864 (1964).

⁷ D.M. Ceperley and B.J. Alder, Phys. Rev. Lett. **45**, 566 (1980); J. P. Perdew and A. Zunger, Phys. Rev. B **23**, 5048 (1981).

⁸ J. P. Perdew, K. Burke, M. Ernzerhof, Phys. Rev. Lett. **77**, 3865 (1996).

- ⁹ V. Olevano and L. Reining, Phys. Rev. Lett. **86**, 5962 (2001).
- ¹⁰ W. Ku and A. G. Eguiluz, Phys. Rev. Lett. **82**, 2350 (1999).
- ¹¹ I. Campillo, A. Rubio and J.M. Pitarke, Phys. Rev. B **59**, 12188 (1999).
- ¹² A. Marini, G. Onida and R. Del Sole, Phys. Rev. B **64**, 195125 (2001).
- ¹³ H. Herenreich and H. R. Phillipp, Phys. Rev. **128**, 1622 (1962).
- ¹⁴ M. A. Cazalilla et al., Phys. Rev. B **61**, 8033 (2000).
- ¹⁵ K. Stahrenberg et al., Phys. Rev. B **64**, 115111 (2001).
- ¹⁶ V. P. Zhukov et al., Phys. Rev. B **64**, 195122 (2001).
- ¹⁷ N. Troullier and J.L. Martins, Phys. Rev. B **43**, 1993 (1991).
- ¹⁸ The Drude plasma frequency ω_D has been calculated using the DFT-LDA states. This is justified as the DFT wavefunctions are not renormalized by the GW corrections and the dispersion of the metallic band close to the Fermi level is poorly affected by QP effects.
- ¹⁹ Local field effects are not included in the present work. However, their influence for noble^{11,12} and transition metals² has been extensively studied and found negligible on both EELS and absorption spectra.
- ²⁰ F. Wooten, *Optical properties of solids* (Academic Press, New York, 1972), pp. 126.
- ²¹ F. Bechstedt et al., Phys. Rev. Lett. **78**, 1528 (1997).
- ²² E.D. Palik, *Handbook of Optical Constants of solids* (Academic Press, New York, 1985).
- ²³ P. Monachesi et al., Phys. Rev. B **64**, 115421 (2001).
- ²⁴ G. Fuster et al., Phys. Rev. B **42**, 7322 (1990).